Pergamon

PII: S0277-5387(96)00580-3

Polyhedron Vol. 16, No. 14, pp. 2381–2386, 1997

0277-5387/97 $17.00+0.00

$[Pt_2(PPh_3)_4(\mu\text{-}S)_2]$ as a metalloligand toward main-group Lewis acids. Crystal structures and bonding analysis of two low-coordinate $BiCl_3$ adducts—$[Pt_2(PPh_3)_4(\mu_3\text{-}S)_2BiCl_3]$ and $[Pt_2(PPh_3)_4(\mu_3\text{-}S)_2BiCl_2]PF_6$

Mei Sheng Zhou,[a] Agnes L. Tan,[b] Yan Xu,[a]† Choon-Fui Lam,[a]
Pak-Hing Leung,[a] K. F. Mok,[a] Lip-Lin Koh[a] and T. S. Andy Hor[a]*

Departments of [a]Chemistry and [b]Computational Science, Faculty of Science, National University of Singapore, Kent Ridge, Singapore 119260

(Received 29 October 1996; accepted 20 November 1996)

Abstract—Addition of $BiCl_3$ to $[Pt_2(PPh_3)_4(\mu\text{-}S)_2]$ gives $[Pt_2(PPh_3)_4(\mu_3\text{-}S)_2BiCl_3]$, which undergoes dissociation and metathesis with NH_4PF_6 to give $[Pt_2(PPh_3)_4(\mu_3\text{-}S)_2BiCl_2]PF_6$. An X-ray single-crystal diffraction analysis established two highly distorted square-pyramidal and tetrahedral structures, respectively. The four- and five-coordination numbers are unusually low among the known Bi^{III} halide adducts. Fenske-Hall MO analysis offers an explanation to the structural characteristics with reference to the stereochemically active lone pairs, coordination numbers, uneven Bi—Cl and Bi—S lengths and the butterfly geometry of the $\{Pt_2S_2\}$ core. These parameters are compared with those of the other intermetallics previously reported. © 1997 Elsevier Science Ltd

Keywords: bismuth; platinum; sulfide; aggregate; metalloligand; heterometallic.

$BiCl_3$ is known to form high-coordinate addition compounds [1], some of which have shown anti-bacterial activities [2]. With a large atomic size and the readily available *d*-orbitals, coordination numbers (C.N.) less than 6 are rare among its coordination complexes. Willey *et al.* have already pointed out that high-coordination geometries are "characteristic traits" of both cationic and anionic Bi^{III} halide complexes [3]. In this paper we wish to demonstrate that the unusual low-coordination complexes can be stabilized by the metalloligand $[Pt_2(PPh_3)_4(\mu\text{-}S)_2]$ [4] (**1**) and that the resultant complexes show some intriguing bonding and geometric properties. The ability of **1** to form intermetallics with *p*-block Lewis acids giving some unexpected structures has been demonstrated in its addition to Tl^I (angular; coordinatively exposed) [5], In^{III} (square-pyramidal; π-bonded to axial Cl) [6], Pb^{II} (trigonal prismatic; structure retention from NO_3^- to PF_6^-) [7] and Ga^{III} (tetrahedral; ion-pair) [5]. Based on the data collected, we can establish some trends of the bonding characteristics of these intermetallics and offer some insights based on Fenske–Hall calculations. A preliminary communication of the activity of **1** toward $BiCl_3$ has been reported [8].

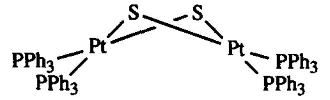

1

RESULTS AND DISCUSSION

Treatment of **1** with equimolar of $BiCl_3$ in MeOH gives $[Pt_2(PPh_3)_4(\mu_3\text{-}S)_2BiCl_3]$ (**2**). Conductivity measurements indicated it to be a non-electrolyte in

---

*Author to whom correspondence should be addressed.

†Present address: Division of Chemistry, National Institute of Education, Singapore 259756.

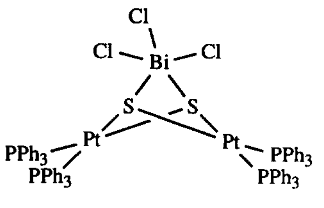

2

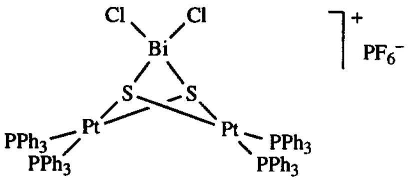

3

CH_2Cl_2, but undergoes partial ionization in MeOH. The ^{31}P NMR spectrum in $CDCl_3$ suggests all the phosphines to be equivalent (δ 16.7 ppm). A high-field shift in CD_3OD (δ 13.9 ppm) is in agreement with chloride dissociation. Metathetic reaction with NH_4PF_6 leads to the isolation of $[Pt_2(PPh_3)_4(\mu_3\text{-}S)_2BiCl_2]PF_6$, (**3**). As these solution data give little information on the geometric characteristics of Bi^{III} and the $\{Pt_2S_2\}$ core, an X-ray crystallographic study was carried out on **2** and **3**.

Complex **2**·CH_2Cl_2 shows a sulfide-bicapped $\{BiPt_2\}$ triangle with negligible Bi—Pt interactions (3.489 Å), (Fig. 1). The local geometry of Bi^{III} is distorted square-based pyramidal (sbp) with Cl(1)—Cl(2)—Cl(3)—S(2) forming the base and S(1) at the axial position. The significantly larger ∡ Cl(3)—Bi—S(2) [160.1(1)°] compared with ∡ Cl(3)—Bi—S(1) [94.5(1)°] and the stronger Bi—S(1) [2.639(3) Å] compared with Bi—S(2) [2.884(3) Å] point to a stereochemically active lone pair *trans* to S(1) [9] (Table 1 & 3). This lone pair also possibly forces an acute chelate bite [∡ S(1)—Bi—S(2) 66.6(1)°], which is the smallest registered among all the intermetallics synthesized. (Table 2) We shall return to these lone pair effects later.

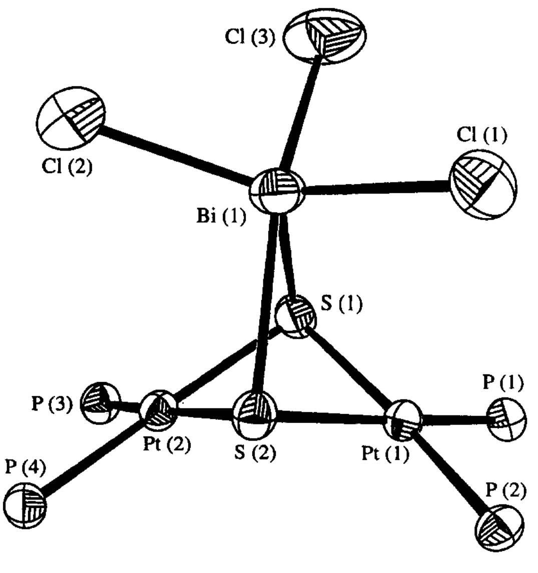

Fig. 1. Molecular structure of $[(PPh_3)_4Pt_2(\mu_3\text{-}S)_2BiCl_3]\cdot CH_2Cl_2$ (**2**) (solvate and phenyl rings removed for clarity).

It is notable that **2** prefers a five-coordinate monomeric form, whereas other $BiCl_3$(S-S) (S-S = bidentate sulfur donors) complexes tend to dimerize through the chloride bridges to give fused-octahedra $(S\text{-}S)Cl_2Bi(\mu\text{-}Cl)_2BiCl_2(S\text{-}S)$, for example, the tetra-*n*-propyldiphosphane disulfide ligand in $[BiCl_3\{Pr^n{}_2(S)P(S)Pr^n{}_2\}]_2$ [3]. Such a tendency for coordination expansion is also found in $BiCl_3L_2$ (e.g. $[BiCl_3(dmso)_2]_n$) [10], $[BiI_4L]^-$ e.g. $[BiI_4(SMe_2)]_2{}^{2-}$ [11] and $[BiX_4]^-$ (X = halide) [12] (e.g. $[BiCl_4]^-$ readily gives $[\{(BiCl_4)_2\}_n]^{2n-}$ [3] and $[BiI_4]^-$ gives $[Bi_3I_{12}]^{3-}$ [13]. The Bi—Cl lengths in **2** are within the range expected for terminal Bi—Cl bonds, but the longest Bi—Cl bond in **2** [Bi(1)—Cl(2) 2.753(4) Å] is significantly longer, and presumably weaker, than many registered terminal Bi—Cl bonds e.g. 2.500(5) and 2.516(5) Å in $[BiCl_3\{Pr^n{}_2(S)P(S)Pr^n{}_2\}]_2$, 2.474(9)–2.528(9) Å in $[(BiCl_4)_2]_n]^{2n-}$ [3], and 2.50(1) and 2.52(1) Å in $[Fe(C_5H_5)_2][BiCl_4]$ [14]. The weakness of this Bi—Cl link provides some justification for its easy dissociation to give **3**, as described earlier.

Although both the local geometries of Bi^{III} in **2** and In^{III} in $[Pt_2(PPh_3)_4(\mu_3\text{-}S)_2InCl_3]$ [5] are square-pyramidal, there are many differences between them. The In^{III} geometry is nearly ideal; it includes both sulfurs on the basal plane with the metal π-bonded to the axial Cl; it is an example of an AB_2X_3-type structure. The Bi^{III} complex (**2**) is severely distorted, with one sulfur at the basal plane and the other in an axial position, and belongs to the AB_2X_3E (E = lone pair) system. The distortion is further aggravated by the close inter- and intramolecular contacts of the phenyl protons to Cl(1) and Cl(2) (2.667 and 2.844 Å) (*cf.* sum of the van der Waal's radii 3.0 Å), which force these two atoms to bend away from the rings and distort from linearly [∡ Cl(1)—Bi—Cl(2) 149.1(1)°].

Complex **3** shows a cationic $\{BiPt_2\}$ complex with uncoordinated $PF_6{}^-$. The four-coordinated Bi^{III} is rare among Bi^{III} coordination complexes. To our knowledge, this is the lowest C.N. ever observed in BiX_3 adducts. The steric demand of the $\{Pt_2S_2\}$ ligand most probably contributes to the stability of the observed low C.N. The local geometry of Bi^{III} is distorted tetrahedral (Fig. 2). With both chlorides and S(1) essentially coplanar with the central Bi, it can also be viewed as a distorted tbp structure with S(2) and the lone pair on the axial plane [15]. Support for this view comes from the significantly strong axial Bi—S(2) bond [2.626(7) Å] compared with the equatorial Bi—S(1) [2.758(7) Å]. Being cationic, and with less bonding ligands, the Bi—Cl and Bi—S bonds are

Table 1. Selected bond distances (Å) and angles (°)

(a) $[Pt_2(PPh_3)_4(\mu_3\text{-}S)_2BiCl_3]\cdot CH_2Cl_2$, (**2**)			
Bi(1)—Cl(1)	2.685(4)	Bi(1)—Cl(2)	2.753(4)
Bi(1)—Cl(3)	2.610(5)	Bi(1)—S(1)	2.639(3)
Bi(1)—S(2)	2.884(3)	Pt(1)—S(1)	2.381(3)
Pt(1)—S(2)	2.344(3)	Pt(1)—P(1)	2.320(3)
Pt(1)—P(2)	2.293(3)	Pt(2)—P(3)	2.302(3)
Pt(2)—P(4)	2.304(4)		
Dihedral angle Pt(1)—S(1)—S(2)—Pt(2)		128.8(3)	
S(1)—Bi(1)—S(2)	66.6(1)	Cl(1)—Bi(1)—Cl(2)	149.1(1)
Cl(1)—Bi(1)—Cl(3)	88.1(1)	Cl(2)—Bi(1)—Cl(3)	87.6(1)
Cl(1)—Bi(1)—S(1)	103.3(1)	Cl(2)—Bi(1)—S(1)	107.5(1)
Cl(1)—Bi(1)—S(2)	90.4(1)	Cl(3)—Bi(1)—S(1)	94.5(1)
Cl(3)—Bi(1)—S(2)	160.1(1)	Cl(2)—Bi(1)—S(2)	103.5(1)
Pt(1)—S(1)—Pt(2)	86.6(1)	Pt(1)—S(2)—Pt(2)	87.8(1)
S(1)—Pt(1)—P(1)	89.1(1)	S(2)—Pt(2)—P(3)	171.4(1)
P(1)—Pt(1)—P(2)	101.1(1)	S(1)—Pt(2)—P(3)	91.9(1)
S(2)—Pt(2)—P(4)	89.0(1)	P(3)—Pt(2)—P(4)	98.8(1)
S(1)—Pt(1)—S(2)	80.0(1)	S(1)—Pt(2)—S(2)	80.4(1)
(b) $[Pt_2(PPh_3)_4(\mu_3\text{-}S)_2BiCl_2]PF_6$ (**3**)			
Bi(1)—Cl(1)	2.464(4)	Bi(1)—Cl(1a)	2.575(4)
Bi(1)—S(1)	2.758(7)	Bi(1)—S(2)	2.626(7)
Pt(1)—S(1)	2.392(7)	Pt(1)—S(2)	2.331(7)
Pt(1)—S(1a)	2.439(7)	Pt(1)—S(2a)	2.311(7)
Bi(1)···Pt(1)	3.432(1)	Bi(1)···Pt(1a)	3.303(1)
Dihedral angle Pt(1)—S(1)—S(2)—Pt(2)		130.7(2)	
S(1)—Bi(1)—S(2)	70.1(2)	Cl(1)—Bi(1)—Cl(1a)	109.1(2)
Cl(1)—Bi(1)—S(1)	133.0(2)	Cl(1a)—Bi(1)—S(1)	117.6(2)
Cl(1)—Bi(1)—S(2)	102.8(2)	Cl(1a)—Bi(1)—S(2)	106.4(2)
S(1)—Pt(1)—S(2)	81.9(2)	Pt(1)—S(1)—Pt(1a)	84.8(2)
Pt(1)—S(2)—Pt(1a)	89.1(2)	S(1)—Pt(1)—P(2)	87.9(2)
S(2)—Pt(1)—P(1)	93.8(2)	P(1)—Pt(1)—P(2)	97.6(1)
S(1a)—Pt(1)—S(2a)	81.2(2)	S(1)—Pt(1)—S(1a)	91.4(2)
P(1)—Pt(1)—S(1a)	82.7(2)	P(2)—Pt(1)—S(2a)	99.1(1)
Bi(1)—S(2)—S(1a)	171.5(9)		

Table 2. Selected structural data for the complex adducts of main-group Lewis acids with $[Pt_2(PPh_3)_4(\mu\text{-}S)_2]$: $[(PPh_3)_4Pt_2(\mu_3\text{-}S)_2GaCl_2][GaCl_4]$ (**A**), $[(PPh_3)_4Pt_2(\mu_3\text{-}S)_2InCl_3]$ (**B**), $[(PPh_3)_4Pt_2(\mu_3\text{-}S)_2Tl][PF_6]$ (**C**), $[(PPh_3)_4Pt_2(\mu_3\text{-}S)_2Pb(NO_3)][NO_3]$ (**D**), $[(PPh_3)_4Pt_2(\mu_3\text{-}S)_2Pb(NO_3)][PF_6]$ (**E**), $[(PPh_3)_4Pt_2(\mu_3\text{-}S)_2BiCl_3]$ (**F**) and $[(PPh_3)_4Pt_2(\mu_3\text{-}S)_2BiCl_2][PF_6]$ (**G**)

Complex	Main-group metal ions M	Ionic radii of M (Å)[a]	Dihedral angles of "Pt_2S_2" (°)	Average bond angles (°) S—M—S	Average bond distances (Å) M—S	Reference
A	Ga^{3+}	0.62	123.1	83.9	2.294	[5]
B	In^{3+}	0.80	128.3	70.8	2.614	[5]
C	Tl^{+}	1.50	135.7	68.9	2.764	[4]
D	Pb^{2+}	1.19	132.2	68.5	2.729	[6]
E	Pb^{2+}	1.19	133.5	69.2	2.693	[6]
F	Bi^{3+}	1.03	128.8	66.6	2.762	This work
G	Bi^{3+}	1.03	130.7	70.1	2.692	This work

[a] Selected from reference [26].

understandably stronger in **3** [mean values of 2.520(4) and 2.692(7) Å, respectively] than in **2** [2.683(4) and 2.762(3) Å, respectively].

Among all the intermetallics known, the $\{Pt_2S_2\}$ moiety is invariably folded along the S···S axis ("*butterfly*"). The nature of this folding appears to be a mix of lattice and electronic factors which are not well-understood to date [16]. When the dihedral angle is plotted against the ionic radii of the heterometal (Fig. 3), a linear relationship is apparent in which the $\{Pt_2S_2\}$ butterfly tends to open up (i.e. flatten) with longer M—S distances and bigger heterometal M.

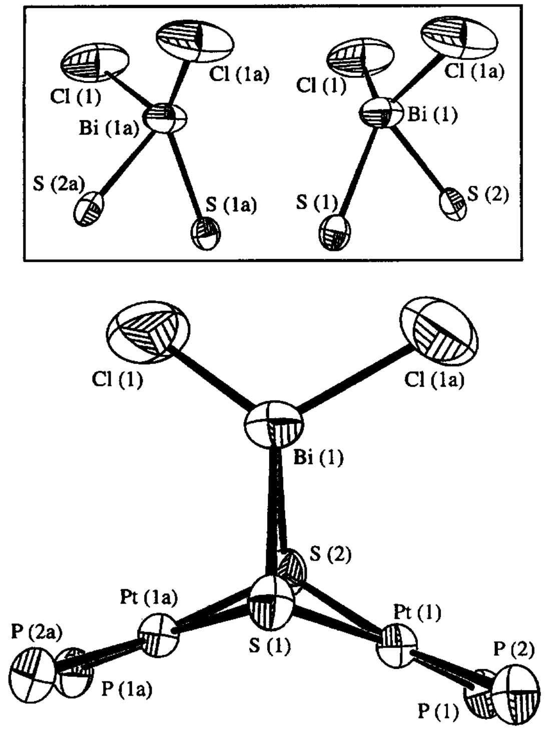

Fig. 2. Molecular structure of $[(PPh_3)_4Pt_2(\mu_3\text{-}S)_2BiCl_2][PF_6]$ (**3**) showing only the molecular cation (phenyl rings removed for clarity). The inset shows two sets of the local structure of Bi^{III} with neighbouring atoms in a disordered model.

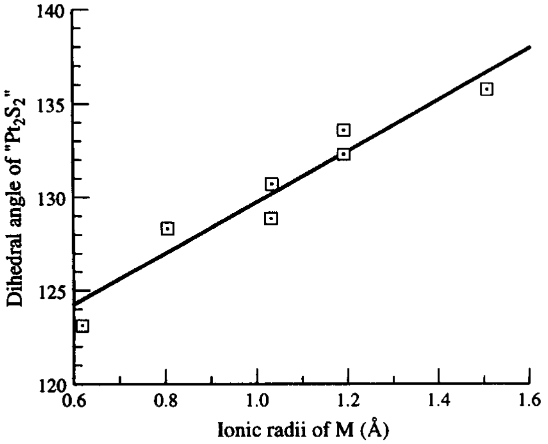

Fig. 3. Plot of the dihedral angle of the hinged $\{Pt_2S_2\}$ core in the intermetallic addition complexes of $[Pt_2(PPh_3)_4(\mu\text{-}S)_2]$ (listed in Table 2) as a function of the ionic radii of the *p*-block metals.

Theoretical calculations [17] have shown that as the dihedral angle decreases, the sulfur lone pairs are increasingly tilted inwards, i.e. toward where the heterometal would be situated [18]. Since the size of M determines the "optimal" orientation of the lone pairs for the M—S interaction, this explains the general trend of increasing dihedral angle with M size (Table 2 and Fig. 3).

The dihedral angle of **2** is smaller than that of **3** [19]. To account for this observation, we invoke a variation of a result obtained previously [20]. The additional Cl ligand in **2** uses a sizeable amount of the Bi p_y orbital [17], such that less of this orbital is available for Bi—S interactions. Consequently, the interactions involve a relatively larger proportion of Bi p_z; this orbital interacts best with the sulfur p_y orbitals. The requisite higher percentage of S p_y in the lone pair orbitals is accomplished by a smaller dihedral angle. We next examine the differences in Bi—S bond lengths [2.639(3) Å and 2.884(3) Å for **2**; 2.626(7) Å and 2.758(7) Å for **3**]. It is likely that the bonds in **2** are longer on average than in **3** because coordination of Cl weakens the Bi—S bonds and **2** has one Cl ligand more. The asymmetric capping of Bi with respect to the two sulfur atoms can be rationalized in terms of competition for orbital interactions: [18] if a ligand is *trans* to a S atom, the associated Bi—S bond would be weakened more than the other. Such a hypothesis is consistent with the structure of **2**, in which one Bi—Cl bond is almost directly *trans* to the longer Bi—S bond. In **3** the longer Bi—S bond is on the side opposite the two Cl ligands; since neither Cl is directly *trans* positioned, the asymmetry in weakening is not as significant.

Previous calculations [18] have demonstrated that the energy involved in binding the Pt_2S_2 moiety to the heterometal fragment is an important determinant of the number of ligands that can be accommodated on the heterometal. Thus, the weakening of the Bi—S bonds on coordination of Cl [21], particularly the long bond in **2**, probably accounts for the low coordination number of Bi: further coordination may weaken the Bi—S bonds to the extent that the binding energy is insufficient for aggregate formation to be sustained.

Regarding the lone pair on Bi, since Bi—S (and Bi—Cl) bonds are stronger than for isoelectronic Pb^{II} and Tl^{I}, the (Bi–ligand antibonding) lone pair has significantly less Bi character (total 31.3% for **2** and 37.2% for **3**, compared with 79.0% and 56.6% for the Tl and Pb compounds, respectively [18]). As such, the lone pair probably imposes less constraints on the coordination geometry of Bi. The character of the lone pair in **2** is 23.4% *s*, 5.8% p_y, 1.1% p_x, 1.5% $d_{x^2-y^2}$ and **3** is 21.4% *s*, 10.7% p_y, 1.2% p_x, 1.5% $d_{x^2-y^2}$. Both are approximately *trans* to the shorter Bi—S bond.

Finally, we comment on the relationship between the coordination geometry of Bi and the two LUMOs when the Cl ligands are absent. The LUMO is mainly p_x and the LUMO2 is $p_x + d_{yz}$; any ligand along the *x* axis also utilizes $d_{x^2-y^2}$, so that two ligands may lie along the *x* axis. [18] The structure of **2** reflects the nature of the LUMOs; in **3** the Cl ligands could be described as being "approximately along the *x* axis", but are skewed to one side of Bi, such that some Bi p_y (and p) can be utilized in Bi—Cl bonding. This skewing results in stronger Bi—Cl interactions (at the expense of Bi—S, as mentioned earlier): in **3** the Bi—Cl bond "more *trans*" to the long Bi—S bond is shorter; the same is true of the Bi—Cl bond directly *trans* to the long Bi—S bond in **2**.

EXPERIMENTAL

All preparations were generally carried out under dry argon and in dry oxygen-free solvents. IR spectra were obtained as KBr discs using a Shimadzu IR-470 spectrometer. Routine ^1H and ^{31}P NMR spectra were recorded at 25°C on a Bruker ACF 300 spectrometer. Conductivities were measured using a Horiba ES-12 conductivity meter. Elemental analyses were performed by the Microanalytical Laboratory in our department.

Complex **1**, $[Pt_2(PPh_3)_4(\mu\text{-}S)_2]$, was synthesized by the standard method from *cis*-$[PtCl_2(PPh_3)_2]$ and $Na_2S \cdot 9H_2O$ [22].

Preparation of $[Pt_2(PPh_3)_4(\mu_3\text{-}S)_2BiCl_3]$ (**2**)

A suspension of $BiCl_3$ (0.047 g, 0.147 mmol) and $[Pt_2(PPh_3)_4(\mu\text{-}S)_2]$ (0.220 g, 0.147 mmol) was stirred in MeOH (50 cm^3) for 3 h to give a clear deep-yellow solution. The solution was filtered and the solvent removed to give an orange residue, which was recrystallized twice from CH_2Cl_2–hexane (yield 0.216 g, 81%). Found: C, 47.5; H, 3.4; Cl, 5.9; P, 6.4; S, 4.2; Pt, 21.7; Bi, 11.9. $C_{73}H_{60}BiCl_5P_4Pt_2S_2$ requires: C, 47.5; H, 3.3; Cl, 5.9; P, 6.8; S, 3.5, Pt, 21.5; Bi, 11.5%. ^{31}P NMR ($CDCl_3$): δ 16.7 [J(P—Pt) = 3154, ^3J(P—Pt) = 15 Hz]. ^{31}P NMR (CD_3OD): δ 13.9 [J(P—Pt) = 3196, ^3J(P—Pt) = 14 Hz]. Molar conductivity Λ_m (CH_3OH, 10^{-3} M): 66.2 Ω^{-1} cm^2 mol^{-1}.

Preparation of $\{[Pt_2(PPh_3)_4(\mu_3\text{-}S)_2]_2BiCl_2\}PF_6$ (**3**).

A MeOH solution of NH_4PF_6 (0.022 g, 0.133 mmol) was slowly introduced to a MeOH solution of **2** (0.241 g, 0.133 mmol). The orange precipitate was filtered, washed with MeOH and recrystallized from CH_2Cl_2–hexane (yield 0.232 g, 91%). Found: C, 44.8; H, 2.9; Cl, 3.0; P, 8.0; S, 3.6; F, 7.6; Pt, 19.6; Bi, 11.0. $C_{72}H_{60}BiCl_2F_6P_5Pt_2S_2$ requires: C, 44.8; H, 3.1; Cl, 3.7; P, 8.0; S, 3.3, F, 5.9; Pt, 20.2; Bi, 10.9%. ^{31}P NMR ($CDCl_3$): δ 13.4 [J(P—Pt) = 3215 Hz]. IR (cm^{-1}): 840 (PF_6^-). Molar conductivity Λ_m (CH_2Cl_2, 10^{-3} M): 56.2 Ω^{-1} cm^2 mol^{-1}.

X-ray crystal structure determination and refinement

Yellow and red prismatic crystals of **2** and **3**, respectively, suitable for single crystal X-ray structure determination were grown by slow diffusion of hexane into the sample solutions in CH_2Cl_2. The crystals of **2** are unstable (with respect to loss of solvate) upon isolation; a crystal of **2** was hence sealed in a quartz capillary with the mother liquor during data collection. Crystals of approximate dimensions 0.30 × 0.30 × 0.25 mm for **2** and 0.25 × 0.25 × 0.40 mm for **3** were used for X-ray diffraction analysis. The unit-cell constants were determined by the least-square-fit to setting parameters of 21 and 18 independent reflections for **2** and **3**, respectively. Detailed crystallographic data are listed in Table 3. A total number of 12,618 ($3.5 < 2\theta < 50°$) for **2** and 5563 ($3.0 < 2\theta < 50°$) for **3** independent reflections were measured by scanning on a Siemens R3M/V2000 diffractometer. The function minimized was $\Sigma w(F_0 - F_c)^2$. The crystal structures were solved by direct methods using the XS program of SHELXTL-

Table 3. Crystallographic data for $[Pt_2(PPh_3)_4(\mu_3\text{-}S)_2BiCl_3] \cdot CH_2Cl_2$ (**2**) and $[Pt_2(PPh_3)_4(\mu_3\text{-}S)_2BiCl_2]PF_6$ (**3**)

Molecular formula	$C_{73}H_{60}BiCl_5P_4Pt_2S_2$ (**2**)	$C_{72}H_{60}BiCl_2F_6P_5Pt_2S_2$ (**3**)
fw	1903.6	1928.2
Space group	$P\bar{1}$	$C2/c$
a (Å)	12.081(2)	21.264(4)
b (Å)	15.225(3)	19.292(4)
c (Å)	20.868(4)	17.303(3)
α (°)	74.32(3)	90
β (°)	86.50(3)	93.11(3)
γ (°)	80.82(3)	90
V (Å^3)	3647(2)	7088(2)
Z	2	4
D_c (g cm^{-3})	1.733	1.807
T (K)	298	298
λ (Mo-K_α) (Å)	0.71073	0.71073
μ (mm^{-1})	6.601	6.718
No. of observed reflections	8009 [$\lvert F_o\rvert > 6.0\sigma(\lvert F_o\rvert)$]	3710 [$\lvert F_o\rvert > 5.0\sigma(\lvert F_o\rvert)$]
R^a	0.036	0.031
$R_w{}^b$	0.040	0.037

$^a R = \Sigma\lvert\lvert F_o\rvert - \lvert F_c\rvert\rvert / \Sigma\lvert F_o\rvert$.

$^b R_w = [\Sigma w(\lvert F_o\rvert - \lvert F_c\rvert)^2 / \Sigma w\lvert F_o\rvert^2]^{1/2}$.

Plus (Siemens Analytical Instruments, Inc. 1989) and refined by full-matrix least-squares analysis with the XLS program (based on SHELXS-76, Sheldrick, 1976). Analytical expressions of neutral-atom scattering factors were employed and anomalous corrections were incorporated [23]. The raw data were processed with the learnt-profile procedure [24] and absorption corrections using a program supplied in the SHELXTL-PC package were applied by fitting a pseudo-absorption ellipsoid to the ψ-scan data for 12–20 selected strong reflections over a range of 2θ angles [25]. The positions of heavier atoms Pt, Bi and S were located first by direct method and all non-hydrogen atoms were refined anisotropically. The hydrogen atoms were placed at calculated positions with fixed isotropic thermal parameters. The structure of **3** was initially refined with the Bi atom sitting on the two-fold axis. This led to a R value of 0.076 with $S = 2.97$ as well as very bad anisotropic thermal parameters for Bi and S atoms. A disordered model with Bi displaced about 0.5 Å from the two-fold axis and the S split into two positions *ca* 0.35 Å apart was then used. With the disorder atoms at 0.5 site occupancy, the model led to a final R of 0.031 and $S = 1.07$, with normal anisotropic thermal parameters. Without disorder, the complex cation has a C_2 symmetry. With disorder, this two-fold symmetry is removed.

Acknowledgements—The authors are thankful to the University for financial support (Grant RP950695), the technical staff of the Chemistry Department for support, A. M. Tan for experimental and Y. P. Leong for stenographic assistance. A.L.T. is grateful to the National Science and Technology Board (Singapore) for a fellowship award and the National Supercomputing Research Center for use of its computing facilities and MSI Cerius2 software.

REFERENCES

1. Hegetschweiler, K., Ghisletta, M. and Gramlich, V., *Inorg. Chem.* 1993, **32**, 2699; Clegg, W., Farrugia, L. J., McCamley, A., Norman, N. C., Orpen, A. G., Pickett, N. L. and Stratford, S. E., *J. Chem. Soc., Dalton Trans.* 1993, 2579; Battaglia, L. P. and Corradi, A. B., *J. Chem. Soc., Dalton Trans.* 1983, 2425; Cavalca, L. and Gasparri, G. F., *Acta Cryst.* 1972, **B28**, 1169.
2. Summers, S. P., Abboud, K. A., Farrah, S. R. and Palenik, G. J., *Inorg. Chem.* 1994, **33**, 88.
3. Willey, G. R., Barras, J. R., Rudd, M. D. and Drew, M. G. B., *J. Chem. Soc., Dalton Trans.* 1994, 3025.
4. Briant, C. E., Hor, T. S. A., Howells, N. D. and Mingos, D. M. P., *J. Chem. Soc., Chem. Commun.* 1983, 1118.
5. Zhou, M., Xu, Y., Koh, L.-L., Mok, K. F., Leung, P.-H. and Hor, T. S. A., *Inorg. Chem.* 1993, **32**, 1875.
6. Zhou, M., Xu, Y., Lam, C.-F., Leung, P.-H., Koh, L.-L., Mok, K. F. and Hor, T. S. A., *Inorg. Chem.* 1994, **33**, 1572.
7. Zhou, M., Xu, Y., Lam, C.-F., Koh, L.-L., Mok, K. F., Leung, P.-H. and Hor, T. S. A., *Inorg. Chem.* 1993, **32**, 4660.
8. Zhou, M., Leung, P.-H., Mok, K. F. and Hor, T. S. A., *Polyhedron* 1996, **15**, 1737.
9. The shorter axial Bi—S(1) is also expected for a five-electron-pair sbp system.
10. Weitze, A., Blaschette, A., Henschel, D. and Jones, P. G., *Z. Anorg. Allg. Chem.* 1995, **621**, 229.
11. Clegg, W., Norman, N. C. and Pickett, N. L., *Polyhedron* 1993, **12**, 1251.
12. Geiser, U., Wang, H. H., Budz, S. M., Lowry, M. J., Williams, J. M., Ren, J. and Whangbo, M.-H., *Inorg. Chem.* 1990, **29**, 1611; Rogers, R. D., Bond, A. H., Aguinaga, S. and Reyes, A., *J. Am. Chem. Soc.* 1992, **114**, 2967.
13. Carmalt, C. J., Farrugia, L. J. and Norman, N. C., *Z. Anorg. Allg. Chem.* 1995, **621**, 47.
14. Mammano, N. J., Zalkin, A., Landers, A. and Rheingold, A. L., *Inorg. Chem.* 1977, **16**, 297.
15. A simple VSEPR approach offers little help with regard to the location of the lone pair due to the constraint imposed by the chelating sulfur ligand on a highly distorted Bi^{III} structure.
16. A recently reported pyridyl (Py)-phosphine derivative $Pt_2(PPh_2Py)_4(\mu\text{-}S)_2$ has a planar $\{Pt_2S_2\}$ core. See Yam, V. W.-W., Yeung, P. K.-Y. and Cheung, K.-K., *J. Chem. Soc., Chem. Comun.* 1995, 267. A related $[Pd_2(dppf)_2(\mu_3\text{-}S)_2(AgCl)_2]$ [dppf = $Fe(C_5H_4PPh_2)_2$] is also planar. See Li, G., Li, S., Tan, A. L., Hor, T. S. A., Yip, W.-H. and Mak, T. C. W., *J. Chem. Soc., Dalton Trans.*, 1996, 4315.
17. The molecules are aligned such that the S···S line is along the y axis, S—Bi—S is in the yz plane and the Pt···Pt line is approximately parallel to the x axis. All phenyl rings on phosphine ligands are replaced by hydrogen atoms. Calculations quoted are of the Fenske–Hall type, using Mulliken population analyses to obtain atomic charges and overlap populations. The only "non-standard" basis functions used were for Bi, which were based on Xα calculations for Bi(+0.6).
18. Tan, A. L., Chiew, M. L. and Hor, T. S. A., *J. Mol. Struct. (TheoChem.)*, in press.
19. The Bi—S—S angles are 60.6 and 52.8° in **2** and 56.9 and 53.0° in **3**. Such structural information alone does not account for the smaller dihedral angle in **2**, based on the result in [18].
20. Liu, H., Tan, A. L., Xu, Y., Mok, K. F. and Hor, T. S. A., *Polyhedron*, 1997, **16**, 377.
21. Based on a hypothetical model used in the calculations in which the Bi atom is free of chlorides.
22. Ugo, R., La Monica, G., Cenini, S., Segre, A. and Conti, F., *J. Chem. Soc. A* 1971, 522.
23. *International Tables for X-ray Crystallography*, Vol. 4. Kynoch Press, Birmingham, U.K., 1974.
24. Diamond, R., *Acta Cryst.* 1969, **A27**, 43.
25. North, A. C. T., Phillips, D. C. and Mathews, F. S., *Acta Cryst.* 1968, **A24**, 351; Kopfmann, G. and Huber, R., *Acta Cryst.* 1968, **A24**, 348.
26. Dean, J. A. (ed.) *Lange's Handbook of Chemistry*, 14th edn. McGraw-Hill, New York, 1992, pp. 4.13–4.17.